Paper

Growth Characteristics of a Cherenkov Laser Filled with Inhomogeneous and Lossy Background Plasma

Non-member Tipyada Thumvongskul (Osaka University)
Member Toshiyuki Shiozawa (Osaka University)

With the aid of the multilayer approximation method, growth characteristics of a Cherenkov free-electron laser filled with background plasma with a transversely inhomogeneous density profile are discussed. The accuracy of numerical results is confirmed by comparison with the available analytical solution. From the numerical results, including the effect of electron-ion collisions, we find a great enhancement in the growth characteristics by a proper choice of various parameters, as compared with the corresponding vacuum device. In addition, we can identify the main parameter of the inhomogeneous background plasma which affects growth characteristics of a plasma-filled Cherenkov laser.

Keywords: Cherenkov laser, high power millimeter wave source, inhomogeneous and lossy plasma

1. Introduction

Relativistic electron beam devices utilizing the induced Cherenkov effect are a potential and novel class of coherent high-power and tunable sources at short millimeter and submillimeter wavelengths [1]~[5]. They have a promising future in various applications, such as space-communications, high-resolution radars, remote sensing, and so forth [6]. In recent years, it has been reported that efficiencies of the vacuum Cherenkov devices can be greatly enhanced by the injection of a dense background plasma [7]~[11]. By the plasma injection scheme, the beam-wave coupling responsible for the Cherenkov interaction is modified in a constructive manner, leading to a significantly improved spatial growth rate and output power. Additionally, several beneficial features of the background plasma also help relax the requirements on beam focusing and ease the operations of devices. For these reasons, the plasma-filled electron devices have become a new research area of tremendous interest.

Nevertheless, in many theoretical works, the background plasma was assumed homogeneous for simplicity of the analysis [8] [11]. Meanwhile, in actual experimental situations, there exists some inhomogeneity in the plasma density owing to diffusion and/or recombination of charged particles. In typical cases, we find the background plasma having a transversely inhomogeneous density with a bell-shaped or parabolic profile (see Fig. 1) [9] [12]. In this work, we investigate the effect of plasma inhomogeneity on the growth characteristics of a two-dimensional (2-D) model of a plasma-filled Cherenkov free-electron laser (CFEL). The analysis is carried out on the basis of the multilayer approximation method [12]. In section 2, we start with a general description of the method. Then, in order to confirm the accuracy of our numerical results, they will be compared with the analytical solution available for a parabolic plasma density profile [13]. In addition, we take into account the effect of electron-ion collisions in plasma, which becomes significant at millimeter wavelengths where the background plasma with densities of $10^{12} \sim 10^{15}\mathrm{cm}^{-3}$ is required [11]. In section 3, we discuss the dispersion and growth characteristics based upon numerical results. From the above results, we can identify the main parameter of the inhomogeneous background plasma which affects the growth characteristics of the CFEL in the context of the spatial growth rates. A brief conclusion is stated in section 4.

2. Multilayer Approximation Method for Inhomogeneous Background Plasma

A 2-D parallel-plate model of a plasma-filled CFEL illustrated in Fig. 1 is considered. A dense background plasma with transverse density profile described by

$$N_p = -\frac{N_{p,peak}}{\left(\frac{a+d}{2}-p\right)^h}\left|y-\frac{a+d}{2}\right|^h + N_{p,peak} \quad \cdots (1)$$

occupies the entire region over the dielectric sheet with

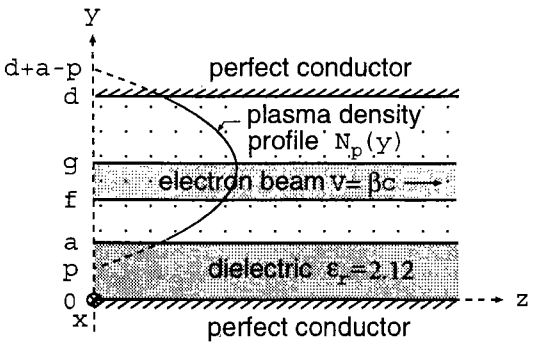

Fig. 1. Geometry of the problem.

relative permittivity ε_r and thickness a through the upper conductor plate located at the distance $d-a$ above the dielectric sheet. In particular, Eq. (1) with $h=2$ corresponds to a parabolic density profile. In the plasma region, a planar relativistic electron beam with initial velocity V and thickness $g-f$ is injected. For simplicity, we assume that both the background plasma and the electron beam are restricted to move only in the z direction by a sufficiently large axial magnetic field.

2.1 Description of the method On the basis of the multilayer approximation method [12], the plasma slab with a transverse density profile described by Eq. (1) can be approximated by n homogeneous layers with different densities as shown in Fig. 2, while the electron beam is assumed homogeneous due to the much lower density. Then, from Maxwell's equations, the relativistic equation of motion for the electron, and the continuity equation [3][8][11], we obtain the wave equations for the TM waves in dielectric, the ith layer of plasma and plasma/beam regions, respectively, as

$$\left(\frac{\partial^2}{\partial y^2}+p_y^2\right)\tilde{E}_z=0$$
$$\left(\frac{\partial^2}{\partial y^2}+k_{y1}^2(y_i)\right)\tilde{E}_z=0$$
$$\left(\frac{\partial^2}{\partial y^2}+k_{y2}^2(y_i)\right)\tilde{E}_z=0 \quad \cdots\cdots\cdots\cdots\cdots (2)$$

where

$$p_y^2=\varepsilon_r\frac{\omega^2}{c^2}-k_z^2\ ,\quad h_y^2=k_z^2-\frac{\omega^2}{c^2}$$
$$k_{y1}^2(y_i)=-\varepsilon_p(y_i)h_y^2\ ,\quad k_{y2}^2(y_i)=-\varepsilon_{pb}(y_i)h_y^2$$
$$\varepsilon_p(y_i)=1-\frac{\omega_p^2(y_i)}{\omega^2}$$
$$\varepsilon_{pb}(y_i)=1-\frac{\omega_p^2(y_i)}{\omega^2}-\frac{\omega_b^2}{\gamma^2(\omega-k_zV)^2}$$
$$\omega_p^2(y_i)=\frac{e^2N_p(y_i)}{\varepsilon_0 m_0}\ ,\quad \omega_b^2=\frac{e^2N_{b0}}{\gamma\varepsilon_0 m_0}$$
$$\gamma=\frac{1}{\sqrt{1-\beta^2}}\ ,\quad \beta=\frac{V}{c}. \quad \cdots\cdots\cdots\cdots (3)$$

Here, $\tilde{E}_z$ is the Fourier amplitude for the axial electric field, and ω, c, ε_0, m_0 and e denote the operating frequency, the velocity of light in vacuum, the permittivity of vacuum, and the rest mass and electric charge of the electron, respectively. The plasma frequencies ω_p and ω_b correspond to the number densities N_p for the background plasma at a certain position y_i in the ith layer and N_{b0} for the electron beam, respectively. Further, k_z is the longitudinal wave number, while p_y, h_y, k_{y1} and k_{y2} are, respectively, the transverse wave numbers in the dielectric, vacuum, plasma and beam regions. From Eq. (2), we can get the solutions for the field components in each region. In the dielectric, since $\tilde{E}_z$ vanishes at the bottom metallic wall, we obtain

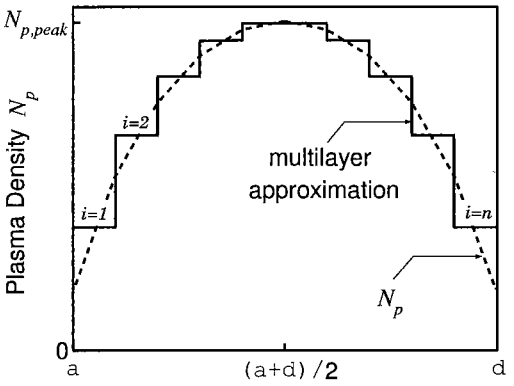

Fig. 2. Plasma density profile in multilayer approximation method.

$$\tilde{E}_z=A\sin p_y y$$
$$\tilde{E}_y=-\mathrm{j}\frac{k_z}{p_y^2}\frac{\partial\tilde{E}_z}{\partial y}$$
$$\tilde{B}_x=\mathrm{j}\frac{\varepsilon_r\omega}{c^2p_y^2}\frac{\partial\tilde{E}_z}{\partial y} \quad \cdots\cdots\cdots\cdots (4)$$

and in the ith layer of plasma or beam region,

$$\tilde{E}_{z,i}=\begin{cases} B_i\sin k_{yi}y_i+C_i\cos k_{yi}y_i & \text{for } \varepsilon_{pi}<0 \\ B_i\sinh k_{yi}y_i+C_i\cosh k_{yi}y_i & \text{for } \varepsilon_{pi}>0 \end{cases}$$
$$\tilde{E}_{y,i}=\mathrm{j}\frac{k_z}{h_y^2}\frac{\partial\tilde{E}_{z,i}}{\partial y}$$
$$\tilde{B}_{x,i}=-\mathrm{j}\frac{\omega}{c^2h_y^2}\frac{\partial\tilde{E}_{z,i}}{\partial y}$$
$$(i=1,2,\ldots,n) \quad \cdots\cdots\cdots\cdots (5)$$

where $\tilde{E}_y$, $\tilde{B}_x$ denote, respectively, the Fourier amplitudes for the transverse electric and magnetic fields, A, B_i and C_i are arbitrary constants, and j is the unit imaginary number. In Eq. (5), k_{yi} and ε_{pi} are equal to $k_{y1}(y_i)$ and $\varepsilon_p(y_i)$ in the plasma region, and equal to $k_{y2}(y_i)$ and $\varepsilon_{pb}(y_i)$ in the beam region, corresponding to their values in the ith layer.

For the boundary conditions at each interface between different mediums or layers, we have

$$\tilde{E}_{z,i}-\tilde{E}_{z,i+1}=0$$
$$\tilde{B}_{x,i}-\tilde{B}_{x,i+1}+\frac{\beta}{c}(\tilde{E}_{y,i}-\tilde{E}_{y,i+1})=0. \quad \cdots\cdots (6)$$

Note that, in the second equation of (6), the third term exists only at the interface that contains a surface current caused by the electron beam. Then, by imposing the above boundary conditions at all the interfaces involved, we eventually obtain

$$\mathbf{D}\cdot\mathbf{A}=\overline{0} \quad \cdots\cdots\cdots\cdots (7)$$

where $\mathbf{A}$ is a column matrix consisting of all the coefficients B_i and C_i, and $\mathbf{D}$ is a square matrix whose elements are functions of frequency and wave number.

For (7) to have a nontrivial solution, the determinant of $\mathbf{D}$ must vanish;

$$\det(\mathbf{D}) = 0. \quad \cdots\cdots\cdots\cdots\cdots\cdots\cdots\cdots \quad (8)$$

Equation (8) corresponds to the dispersion relation which reveals coupling between the negative-energy space-charge wave propagated along the relativistic electron beam and the slow EM wave propagated along the dielectric loaded waveguide filled with plasma. The dispersion relation (8) can be solved numerically for the wave number k_z at a certain frequency. Details in algorithm used to solve Eq. (8) can be seen in [5]. The wave number k_z is a real number when neither gain nor loss exists in the waveguide, but it becomes a complex number of which the imaginary part represents a spatial growth rate α (caused by the beam-wave coupling in a particular range of frequencies) or damping constant (caused by collisions in the plasma).

2.2 Comparison with analytical solution for a parabolic density profile In order to confirm the accuracy of numerical results obtained by the multilayer approximation method, we compare those results with available analytical solutions. For a parabolic density profile ($h = 2$ in Eq. (1)), we can analytically find the expressions for the field components in the plasma slab in the absence of the electron beam in terms of Kummer function [13]. The axial field E_z in the plasma region can be expressed by

$$\tilde{E}_z(y) = \{A\Phi(r1, r2, t) + yB\Phi(r3, r4, t)\}\ \mathrm{e}^{-t/2} \quad \cdots \quad (9)$$

with

$$r1 = \frac{1}{4}\left(1 + \frac{h_y\omega\varepsilon_{p,peak}}{\omega_{p,peak}}\left(\frac{d+a}{2} - p\right)\right),\ r2 = \frac{1}{2}$$

$$r3 = \frac{1}{4}\left(3 + \frac{h_y\omega\varepsilon_{p,peak}}{\omega_{p,peak}}\left(\frac{d+a}{2} - p\right)\right),\ r4 = \frac{3}{2}$$

$$t = h_y\frac{\omega_{p,peak}}{\omega}\frac{(y-(d+a)/2)^2}{(d+a)/2-p} \quad \cdots\cdots\cdots \quad (10)$$

where A and B are arbitrary constants, and Φ denotes a Kummer function

$$\Phi(a,b,x) = 1 + \frac{a}{b}\frac{x}{1!} + \frac{a(a+1)}{b(b+1)}\frac{x^2}{2!} + \frac{a(a+1)(a+2)}{b(b+1)(b+2)}\frac{x^3}{3!} + \cdots \quad \cdots \quad (11)$$

The dispersion relation obtained on the basis of the above analytical expression can be solved for k_z at a certain frequency. In Fig. 3, we show the normalized values of k_z versus the number of plasma layers n calculated for our model in the absence of the electron beam from the two approaches. When $n \geq 20$, the values of $k_z a$ obtained from the multilayer approximation method have relative errors less than 0.001%, and they gradually converge to the exact values as n increases. Hence, with a sufficiently large n, the multilayer approximation method gives a stable solution, and is expected to be applicable to the plasma slab with an arbitrary density profile without significant computational errors. As will be seen later, a very small change in $\mathrm{Re}[k_z]$ yields a relatively large change in α. Therefore, sufficiently small errors confirmed in this step can be useful as a guarantee for accurate numerical results in the next section. For this reason, the value $n = 30$ will be adopted throughout the rest of this paper.

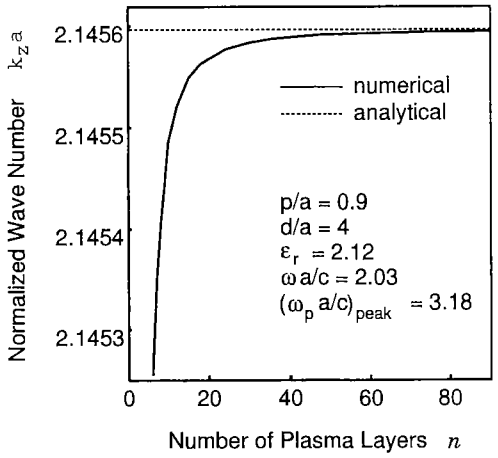

Fig. 3. Normalized wave number $k_z a$ for the lowest-order TM mode versus the number of plasma layers n.

2.3 Effect of electron-ion collisions in the background plasma In many cases where the background plasma has a very large density, we could not possibly ignore the collision between electrons and ions in the plasma. The effect of electron-ion collisions can be taken into account via the collision frequency ν_{ei}. By replacing ε_p and ε_{pb} described in (3) by [11] [14],

$$\varepsilon_p = 1 - \frac{\omega_p^2}{\omega(\omega - \mathrm{j}\nu_{ei})}$$

$$\varepsilon_{pb} = 1 - \frac{\omega_p^2}{\omega(\omega - \mathrm{j}\nu_{ei})} - \left\{\frac{\omega_b}{\gamma(\omega - k_z V)}\right\}^2, \quad \cdot \quad (12)$$

we can yet numerically calculate the eigen value for the complex wave number from the dispersion relation.

The value of ν_{ei} can be estimated by the absolute temperature T and density N of the background plasma [14],

$$\nu_{ei} = \frac{5.5\ N}{T^{3/2}}\ln\left(\frac{220\ T}{N^{1/3}}\right) \quad \cdots\cdots\cdots\cdots\cdots \quad (13)$$

where the ratio ν_{ei}/ω is of the order of 10^{-2} for our model at millimeter wavelengths. The introduction of ν_{ei} into the dispersion relation brings damping (exponential attenuation) to the EM wave for the waveguide without electron beam, as well as degradation in growth characteristics in the process of beam-wave coupling. However, as will be shown in the next section, with a proper choice of various parameters, the spatial growth rate in plasma devices can yet have the values over that for the vacuum device.

3. Numerical Results

Relations between the beam velocity and operating frequency are illustrated in Fig. 4. The lowest curve labeled (a) is that for a typical vacuum device, whereas

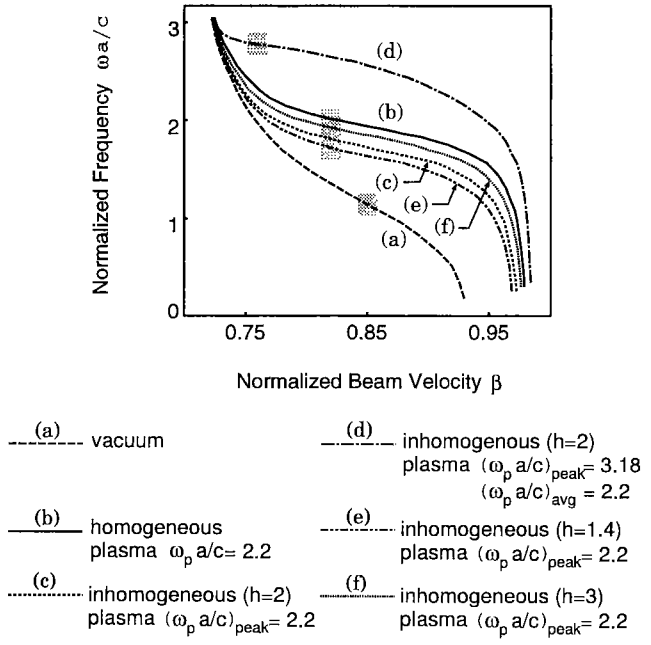

Fig. 4. Operating frequency versus normalized beam velocity β.

the others are for plasma-filled devices. The curves labeled (b), (c), (e) and (f) are for the case where the peak value of plasma frequency $\omega_{p,peak}$ is equal to 2.2ω, and the curve (d) is for $\omega_{p,peak} = 3.18\omega$. Other parameters used in the numerical calculations are shown in Table 1. From this figure, we see that at the same frequency, it is possible in the plasma devices to use the electron beam with higher velocity (or higher current) for which a higher output power can be expected. Also note that the real part of k_z used to determine the phase velocity of the EM wave can be also approximated by $\mathrm{Re}[k_z]=\omega/\beta c$, since for an effective interaction the velocity synchronism should be maintained between the EM wave and the electron beam. Moreover, the values of $\mathrm{Re}[k_z]$ are almost identical to those in the waveguide without the electron beam. Further, the introduction of small $\nu_{ei}(\sim 10^{-2}\omega)$ into the dispersion relation does not affect much the values of β or $\mathrm{Re}[k_z]$. Therefore, we can point out hereby that stable relations between ω and β (or $\mathrm{Re}[k_z]$) can be obtained even in the presence of small values of gain or loss.

We show in Fig. 5 the numerical results of the spatial growth rate $\alpha=\mathrm{Im}[k_z]$ for the beam-wave coupling. The labels (a), (b), (c) and (d) in Fig. 5 corresponds to those in Fig. 4. As is obvious from the figure, the spatial growth rate is greatly enhanced beyond that for the vacuum device by the injection of the background plasma in the CFEL. Especially, in the case of inhomogeneous plasma, the EM field component which interacts with the electron beam can have almost a flat distribution over the cross section of the beam. In this case, we can have a more enhanced growth rate, and a more stable interaction. Nevertheless, when the effect of electron-ion collisions in the background plasma is taken into account, the spatial growth rates are poorly dropped, while the values of $\mathrm{Re}[k_z]$ are almost unchanged, being the same as those shown in Fig. 4. However, with a proper choice of various parameters, we can yet expect that the spatial growth rates in the plasma devices are enhanced beyond those of the corresponding vacuum device.

Table 1. Values of parameters used in numerical simulation.

Waveguide	
Separation between two conducting plates d/a	4.0
Relative permittivity ε_r	2.12
Background Plasma	
Peak plasma frequency $\omega_{p,peak}a/c$	2.2, 3.18
Electron beam	
Dielectric-beam gap $(f-a)/a$	0.85
Beam thickness $(g-f)/a$	0.3
Plasma frequency $\omega_b a/c$	0.0075
Drift velocity β	0.73~0.97

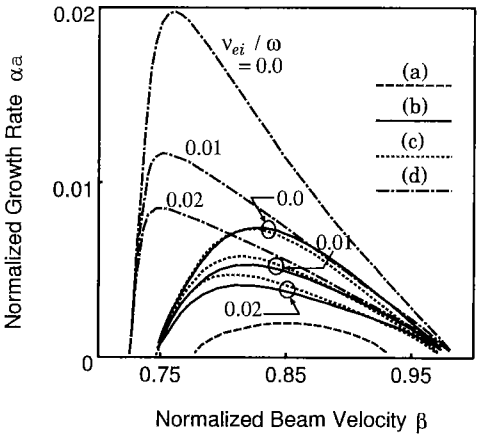

Fig. 5. Spatial growth rate versus normalized beam velocity β for various values of ν_{ei}.

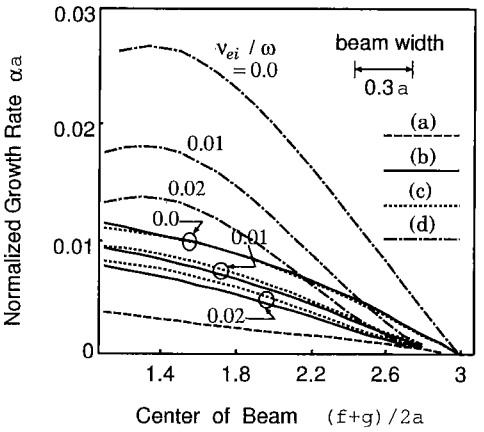

Fig. 6. Spatial growth rate versus beam position for various values of ν_{ei}.

Fig. 6 illustrates the value of α as a function of beam position. The labels (a), (b), (c) and (d) in Fig. 6 corresponds to those in Fig. 4. For each curve, a particular set of ω and β which provides a peak value for α is used. It should be noted that in the shaded areas in Fig. 4

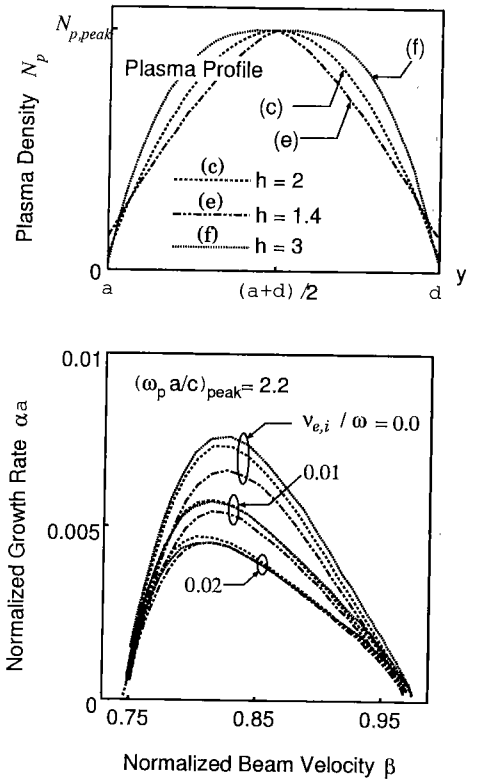

Fig. 7. Spatial growth rate versus normalized beam velocity β for various plasma density profiles.

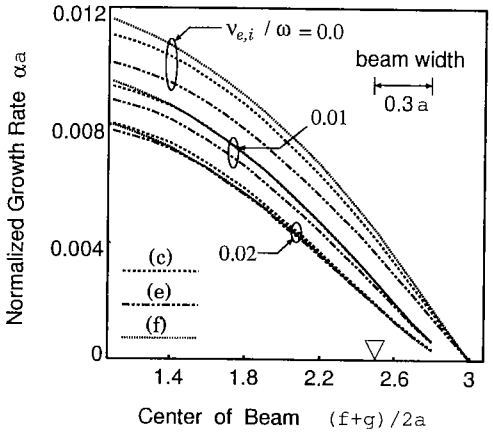

Fig. 8. Spatial growth rate versus beam position for various plasma density profiles. The mark $\triangledown$ indicates the position at which the background plasma has a peak value.

where the values for ω and β are selected, all curves have the most gentle slope. (See also more explanation about a relation between the peak value of α and dispersion feature in [11].) From numerical results, we see that spatial growth rates have very large values when the beam is injected close to the dielectric sheet, but this is not practical. In our calculations for α in Fig. 5, we located the center of the beam at $y = 2a$. We also find in Fig. 6 that the values of α for the plasma devices drop rather steeply when the beam position is far from the dielectric sheet, especially in the case (d) where $\omega_{p,peak} = 3.18\omega$. Thus, a high value of ω_p does not necessarily guarantee the best performance. The most important subject is to select a set of parameters carefully. For example, we should choose a position suitable for the beam alignment which brings a required value of α, or a proper condition for temperature control for which the value of ν_{ei} varies only slightly around an acceptable level.

Next, we consider the effect of plasma inhomogeneity on the growth characteristics of the plasma-filled CFEL. From Figs. 5 and 6, in the case (c) where the inhomogeneous plasma with a parabolic density profile has the peak value of plasma frequency $\omega_{p,peak}$ (or density $N_{p,peak}$) equal to that for the homogeneous case (b), the spatial growth rate slightly deviates from that for (b). However, in the case (d) where the plasma density is increased from the case (c) so that the average value of ω_p equals that for the case (b), the spatial growth rate is greatly raised. We can therefore judge that the main parameter of the background plasma which affects the value of the spatial growth rate is not the average plasma density, but the peak value. This issue is confirmed by the investigation of the growth characteristics for various plasma profiles with the same peak density. Results in Fig. 7 (the labels (c), (e) and (f) in Fig. 7 corresponds to those in Fig. 4) indicate that differences in plasma density profile do not affect much the growth characteristics of the plasma-filled CFEL, provided that the peak values of plasma density are the same. Fig. 8 (the labels (c), (e) and (f) in Fig. 8 corresponds to those in Fig. 4) shows that such results are not because the electron beam passes through the interaction space at the place where the background plasma has the same density. Back to Fig. 4 again, we see that the dispersion characteristics are also not very different for the cases (b), (c), (e) and (f), and the peak values of α take place at about the same value of β (indicated by the biggest shaded box). Consequently, for simplified analysis, we can properly treat the inhomogeneous background plasma as homogeneous with a plasma density equal to the peak value.

4. Conclusion

Growth characteristics of a CFEL filled with a transversely inhomogeneous plasma were investigated with the aid of the multilayer approximation method. The accuracy of the numerical results was confirmed by comparison with the available analytical solution. From the numerical results for growth characteristics, including the effect of electron-ion collisions, we find a great enhancement in the growth characteristics by a proper choice of various parameters, as compared with the corresponding vacuum device. It was also shown that the main parameter of the inhomogeneous background plasma which affects the growth characteristics of the device is the peak plasma density, which can be used for a simplified analysis.

In this work, we investigated the effect of plasma inhomogeneity on the CFEL, in which a dielectric waveguide is used for the slow-wave structure. However, sim-

ilar results can also be expected for the Smith-Purcell free-electron laser which uses the slow-wave structure composed of a metallic grating.

Acknowledgment

The authors would like to thank Prof. G. I. Zaginaylov, Kharkov National University, Ukraine, and Dr. A. Hirata, Osaka University, Japan, for their valuable comments on this work.

(Manuscript received January 26, 2001, revised June 15, 2001)

References

(1) J. E. Walsh, T. C. Marshall, and S. P. Schlessinger, "Generation of coherent Cerenkov radiation with an intense relativistic electron beam," *Phys. Fluids*, vol. 20(4), pp. 709-710 (1977).

(2) J. M. Wachtel, "Free-electron lasers using the Smith-Purcell effect," *J. Appl. Phys.*, vol. 50(1), pp.49-56 (1979).

(3) T. Shiozawa, and T. Nakashima, "Two-dimensional mode analysis of the Raman-type free-electron laser," *J. Appl. Phys*, vol. 55, pp. 637-646 (1984).

(4) J. E. Walsh, T. L. Buller, B. Johnson, G. Dattoli, and F. Ciocci, "Metal-grating far-infrared free-electron lasers," *IEEE J. Quantum Electron.*, vol. QE-21, pp. 920-923 (1985).

(5) T. Shiozawa, and H. Kondo, "Mode Analysis of an open-boundary Cerenkov laser in the collective regime," *IEEE J. Quantum Electron.*, vol. QE-23, pp. 1633-1641 (1987).

(6) A. V. Gaponov-Grekhov, and V. L. Granatstein, Eds., *Applications of High-Power Microwave* (Norwood, MA: Artech House, 1994).

(7) Y. Carmel, K. Minami, R. A. Kehs, W. W. Destler, V. L. Granatstein, D. Abe, and W. L. Lou, "Demonstration of efficiency enhancement in a high-power backward-wave oscillator by plasma injection," *Phys. Rev. Lett.*, vol. 62, pp. 2389-2392 (1989).

(8) H. Kosai, E. P. Garate, and A. Fisher, "Plasma-filled dielectric Cherenkov maser," *IEEE Trans. Plasma Sci.*, vol. 18(6), pp. 1002-1107 (1990).

(9) A. G. Shkvarunets, S. Kobayashi, J. Weaver, Y. Carmel, J. Rodgers, T. M. Antonsen, Jr., V. L. Granatstein, and W. W. Destler, "Electromagnetic properties of corrugated and smooth waveguides filled with radially inhomogeneous plasma," *IEEE Trans. Plasma Sci.*, vol. 24(3), pp. 905-917 (1996).

(10) G. S. Nusinovich, Y. Carmel, T. M. Antonsen, D. M. Goebel, and J. Santoru, "Recent progress in the development of plasma-filled traveling-wave tubes and backward-wave oscillators," *IEEE Trans. Plasma Sci.*, vol. 26(3), pp. 628-645 (1998).

(11) T. Thumvongskul, A. Hirata, G. Zaginaylov and T. Shiozawa, "Enhancement of amplification characteristics in a plasma-filled Cherenkov laser at millimeter wavelengths," *J. Appl. Phys.*, vol. 87(4), pp. 1626-1631 (2000).

(12) S. Pasquiers, "Plasma waves in a bounded anisotropic plasma: influence of the electron density inhomogeneity," *J. Appl. Phys.*, vol. 67(12), pp. 7246-7253 (1990).

(13) G. I. Zaginaylov, "Spectrum of oblique Langmuir waves in an inhomogeneous magnetized plasma waveguide," *Tech. Phys.*, vol. 40(6), pp. 542-545 (1995).

(14) V. L. Ginzburg, *Electromagnetic waves in plasmas* (Pergamon press ltd., 1964).

Tipyada Thumvongskul (Non-member) was born in Bangkok, Thailand, on March 22, 1975. She received the B.E. degree in electrical engineering from Chulalongkorn University, Bangkok, Thailand, in 1996, and the M.E. degree in electrical communication engineering from Osaka University, Osaka, Japan, in 1999. She is now working toward the Ph.D. degree at Osaka University. Her current research field are the free-electron lasers, periodic structures and waveguide discontinuities.

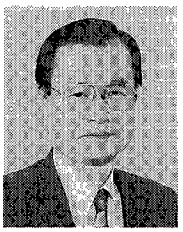

Toshiyuki Shiozawa (Member) was born in Tokyo, Japan, on January 16, 1941. He received the B. E., M. E. and Ph. D. degrees in electrical communication engineering from Osaka University, Suita, Osaka, Japan in 1964, 1966 and 1969, respectively. In 1969 he joined the Department of Communication Engineering, Osaka University, where he is now a Professor.

He has been engaged in the research of relativistic electromagnetic theory for engineering-oriented applications, and theoretical study of free-electron lasers. His current research interests include nonlinear electromagnetics and bioelectromagnetics. He has been serving as a member of the Editorial Boards of the IEEE Transactions on Microwave Theory and Techniques since 1987 and the Journal of Applied Physics since 1984. He served also as an Associate Editor of the IEICE Transactions on Electronics from 1995 to 1999. He is the Chairman of the Technical Committee on Electromagnetic Theory in IEE Japan. In 2000, he organized the Japan-China Joint Meeting on Optical Fiber Science and Electromagnetic Theory. He is a co-author of the books *Topics in Advanced Electromagnetic Theory* (Tokyo, Japan: Corona, 1988) and *Exercise in Electromagnetic Theory* (Tokyo, Japan: Corona, 1998). In 2001, he was elected to the grade of IEEE Fellow for contributions to engineering-oriented relativistic electromagnetic theory and theoretical study of free-electron lasers.

Dr. Shiozawa is a member of the Institute of Electronics, Information and Communication Engineers.